

An Unsupervised Fuzzy Clustering Approach for Early Screening of COVID-19 From Radiological Images

Weiping Ding¹, Senior Member, IEEE, Shouvik Chakraborty², Member, IEEE, Kalyani Mali, Sankhadeep Chatterjee³, Janmenjoy Nayak⁴, Asit Kumar Das⁵, and Soumen Banerjee⁶, Senior Member, IEEE

Abstract—A global pandemic scenario is witnessed worldwide owing to the menace of the rapid outbreak of the deadly COVID-19 virus. To save mankind from this apocalyptic onslaught, it is essential to curb the fast spreading of this dreadful virus. Moreover, the absence of specialized drugs has made the scenario even more badly and thus an early-stage adoption of necessary precautionary measures would provide requisite supportive treatment for its prevention. The prime objective of this article is to use radiological images as a tool to help in early diagnosis. The interval type 2 fuzzy clustering is blended with the concept of superpixels, and metaheuristics to efficiently segment the radiological images. Despite noise sensitivity of watershed-based approach, it is adopted for superpixel computation owing to its simplicity where the noise problem is handled by the important edge information of the gradient image is preserved with the help of morphological opening and closing based reconstruction operations. The traditional objective function of the fuzzy c-means clustering algorithm is modified to incorporate the spatial information from the neighboring superpixel-based local window. The computational overhead associated with the processing of a huge amount of spatial information is reduced by incorporating the concept of superpixels and the optimal clusters are determined by a modified version of the flower pollination algorithm. Although the proposed approach performs well but should not be considered as an alternative to gold standard detection tests of COVID-19.

Experimental results are found to be promising enough to deploy this approach for real-life applications.

Index Terms—COVID-19, interval type-2 fuzzy system, radiological image segmentation, unsupervised fuzzy clustering.

I. INTRODUCTION

THE NOVEL Coronavirus disease or COVID-19 is truly a petrifying and epic crisis that possess one of the biggest threats to mankind in recent times. Although the mortality rate is not very high, the absence of any dedicated drugs has worsened the situation further. It is an utmost necessity to detect the presence of infection in the human body as early as possible. Thus, early detection is one of the key precautionary measures to restrict the drastic spread of this highly infectious virus and to save many lives. These causes led to the wide increase in the popularity of automated systems to detect or help in the detection of the presence of COVID-19 infection. Although detection does not necessarily guarantee a complete cure, however, it is highly useful in providing supportive treatments to infected patients as well as to isolate suspected patients from the rest of the community [1], [2]. Although Reverse transcription-polymerase chain reaction is considered as one of the gold standards worldwide in the detection of the presence of COVID-19 virus, however, it is quite time-consuming (approximately 4 to 8 h). Moreover, this test can only be performed through the collection of nasopharyngeal swabs or deep-throat saliva. On the other hand, chest CT scans or X-Rays show some vital patterns that can be a hint of COVID-19 infection.

The visual diagnosis of COVID-19 infection involves examining CT or X-Ray images of the chest region that are collected from the suspected patients by a physician or domain expert. Evaluation of the visual features may not always reveal the type of infection accurately but if it is attributed to COVID-19 infection, then precautionary measures can always be initiated and supportive treatments can be provided to the suspect.

There are several approaches reported in the literature that tries to detect the presence of the COVID-19 virus from chest CT scans and/or X-ray images. In most of the recent works [3]–[14], the deep learning approach is adopted to automatically classify the images [15], [16]. In [17], a deep learning-based model is proposed to automatically segment and classify the COVID-19

Manuscript received May 18, 2021; revised June 29, 2021; accepted July 12, 2021. Date of publication July 19, 2021; date of current version August 4, 2022. The work of W. Ding was supported in part by the National Natural Science Foundation of China under Grants 61300167 and 61976120, in part by the Natural Science Foundation of Jiangsu Province under Grant BK20191445, in part by the Natural Science Key Foundation of Jiangsu Education Department under Grant 21KJA510004, and in part by the Qing Lan Project of Jiangsu Province. (Corresponding authors: Sankhadeep Chatterjee; Asit Kumar Das.)

Weiping Ding is with the School of Information Science and Technology, Nantong University, Nantong 226019, China.

Shouvik Chakraborty and Kalyani Mali are with the Department of Computer Science and Engineering, University of Kalyani, Kalyani 741235, India.

Sankhadeep Chatterjee is with the Department of Computer Science and Engineering, University of Engineering and Management, Kolkata 700160, India.

Janmenjoy Nayak is with the Department of Computer Science and Engineering, Aditya Institute of Technology and Management, Srikakulam 532201, India.

Asit Kumar Das is with the Department of Computer Science and Technology, Indian Institute of Engineering Science and Technology, Howrah 711103, India (e-mail: akdas@cs.iests.ac.in).

Soumen Banerjee is with the Department of Electronics and Communication Engineering, University of Engineering and Management, Kolkata 700160, India.

Color versions of one or more figures in this article are available at <https://doi.org/10.1109/TFUZZ.2021.3097806>.

Digital Object Identifier 10.1109/TFUZZ.2021.3097806

CT scan images. The approach utilizes multitask deep learning to achieve better performance as compared to U-Net architecture by exploiting the information content of multiple tasks. A lung X-ray image segmentation approach proposed in [18] uses multiple transfer learning to effectively segment lung lesions from low-quality X-ray images. The method is so designed to be deployed with portable X-ray imaging devices. Its main objective is to support physicians in analyzing X-ray images automatically from portable devices that generally produce poor-quality images. Another deep neural network-based automated COVID-19 CT image and X-Ray image analysis method is proposed in [19]. Herein multitask pipeline is used to exploit the advantages of the deep-learning approach. The proposed method is an enhancement of the Inception-v3 deep learning model through the adoption of a multi-modal learning approach with experimental results depicting 99.4% accuracy. Another approach that detects the severity of COVID-19 infection from chest X-Ray images is reported in [20]. Here lung segmentation and opacity detection from chest CT images can be performed and experiments were carried out on 48 COVID-19 positive patients with encouraging outcomes. In [21], automatic lung infection segmentation is proposed. This approach, based on a deep neural network and termed as Inf-Net, is applied to the chest CT images. It can effectively segment the infected lung region from the chest CT scan images by generating a global map with the help of a parallel partial decoder. This semisupervised approach is proven to achieve better learning ability and outperforms many state-of-the-art segmentation approaches. An unsupervised lung CT segmentation approach is proposed in [22]. This approach uses the representational learning approach and clustering and can segment the infected regions from the lung CT volumes. Experimental results prove that this approach is efficient enough and can effectively segment the infected region of the lung CT volume. A superpixel-based radiological image interpretation approach is proposed in [23]. This approach is helpful in the early diagnosis of the COVID-19. The cuckoo search approach is modified by incorporating the Luus–Jaakola heuristic and McCulloch’s approach. The fuzzy objective function is modified to exploit the advantages of the superpixels. This approach is promising enough to be applied in real-life applications. Morphology-based radiological image segmentation approach is proposed in [24]. This approach exploits the advantages of simple morphological operations and it is useful in the early screening of the COVID-19 infection. This approach is evaluated using some standard evaluation matrices and the performance is found to be quite satisfactory. Some comprehensive reviews of the application of artificial intelligence and machine learning techniques in different phases of COVID-19 image processing can be found in [25]–[28].

In this article, the application of artificial intelligence and machine learning in image acquisition, analysis, and segmentation is illustrated which is helpful in the diagnosis process. As discussed, although much effort has been dedicated to computer vision and artificial intelligence for pneumonia and COVID-19 diagnosis, yet it can be noted that most of the discussed approaches require at least some labeled images to get trained. Herein lays the problem that the amount of the labeled

samples is very less. Still, literature on supervised learning-based COVID-19 detection using CT or X-Ray images is growing significantly. It can also be observed from the present state-of-the-art literature, that the unsupervised approaches are not investigated rigorously even though they can be quite helpful on various occasions [29]–[31]. Motivated from this, an image analysis process is proposed in this article that is not dependent on any pre-labeled data. The proposed work is basically a segmentation procedure that helps to easily identify different regions of the chest CT or X-Ray images that is essential in easy and precise diagnosis. The proposed approach can work without any manual delineation. Although it is always better to compare the results of any segmentation approach with the manual delineations that are performed by the domain experts, in this case, it is very difficult to engage a domain expert to make manual segmentation [32]. Hence, besides qualitative evaluation, the proposed approach is evaluated using some standard validity indices that are helpful to measure the performance of the proposed method quantitatively.

In recent years, biomedical image segmentation incorporates fuzzy logic systems to enhance the quality of the segmentation outcome by representing the spatial information efficiently [33], [34]. In most of the scenarios, it is observed that the fuzzy clustering systems achieve a better yield as compared to the traditional crisp clustering approaches. It is mostly due to the uncertainty modeling capability of fuzzy systems. Type-2 fuzzy logic approaches have become very popular nowadays that replace the type-1 fuzzy logic techniques on many occasions. Typically type-2 fuzzy systems can more efficiently handle the uncertainty compared to that of type-1 fuzzy systems because the latter uses a scalar membership whereas the former uses a fuzzy membership function [35], [36]. This additional degree of fuzziness helps to conveniently handle the uncertainty compared to type-1 fuzzy techniques. It is also experimentally proven that the type-2 fuzzy technique is useful in determining the threshold value that can be associated with segmentation purposes [37]. Inspired by this fact, the type-2 fuzzy logic system is adopted in this article to segment the chest CT and X-ray images to help early and easy understanding of the COVID-19 infection. The interval type-2 fuzzy logic system is hybridized with the superpixels and the modified flower pollination approach [38]. The incorporation of the concept superpixel renders reduction of computational overhead and helps in providing an efficient way of representing spatial information. The flower pollination algorithm developed by Yang [39] is successfully applied to solve various problems [40] like various other metaheuristics [31], [41]. For the sake of conciseness of the article, the authors have refrained themselves from illustrating this approach in detail with appropriate citations added for further references. The proposed approach updates the cluster centers with the help of an enhanced flower pollination algorithm and avoids incorporation of equations for further cluster center updation purpose. The modification mainly incorporated in the modified flower pollination approach is the enhancement in the local pollination method to improve the performance of segmentation. The details of the fuzzy objective function are given in the following section.

Thus, to summarize, the main contributions of this article are as follows.

- 1) A novel superpixel-based segmentation approach is proposed that reduces the computational cost for processing lots of spatial information.
- 2) The modified flower pollination algorithm is used to determine the optimal clusters that replace the updated process of traditional interval type-2 fuzzy cluster center.
- 3) The traditional objective function of the fuzzy c-means clustering algorithm is modified to incorporate the local spatial information from the neighboring superpixel-based spatial window.

These are some of the major contributions from the algorithmic perspective. Apart from these contributions, the main contribution of this article lies in the early screening of the COVID-19 infected/suspected patients. The proposed approach will serve as a tool for the physicians in accurate interpretation of the radiographic images. The proposed approach can efficiently segment the input images. The segmented outcomes will be helpful in the easy interpretation of the radiographic images. Hence, the proposed approach can be adopted as an expert system that can be helpful in easy and early detection of the COVID-19 suspects and the confirmation can be obtained by some standard tests later on.

The organization of the rest of the article is as follows: Section II illustrates the proposed approach along with the necessary background information in detail. Section III presents the experimental outcomes and Section IV discusses comprehensive analysis. Finally, Section V concludes this article.

II. PROPOSED APPROACH

A. Overview of Type-2 Fuzzy Sets and Interval Type-2 Fuzzy Sets

The type-2 fuzzy sets, also known as the ultrafuzzy sets [42] are distinguished from type-1 fuzzy sets by a type-2 membership function $\mu_S(x, v)$, where $x \in X$, and $v \in J_x \subseteq [0, 1]$. Here, S denotes a type-2 fuzzy set and can be expressed by (1). The interval type 2 fuzzy sets are a specific type of the type-2 fuzzy systems

$$\hat{S} = \{((x, v), \mu_S(x, v)) \mid \forall x \in X, \forall v \in J_x \subseteq [0, 1]\}. \quad (1)$$

Here, $\mu_S(x, v)$ denotes the type-2 fuzzy membership function and the range of it are given as $0 \leq \mu_S(x, v) \leq 1$. An alternate definition of type-2 fuzzy sets is given as

$$S = \int_{x \in X} \int_{v \in J_x} \mu_S(x, v)/(x, v), J_x \in [0, 1]. \quad (2)$$

Here, the union operation over all permissible x and v is denoted by $\int \int$ due to the continuous universe of discourse. It can be noted that in discrete universe of discourse, the same union operator can be replaced with $\sum \sum$. It is interesting to observe that, if all the uncertainty vanishes then the type-2 membership function gets reduced to the type-1 membership function.

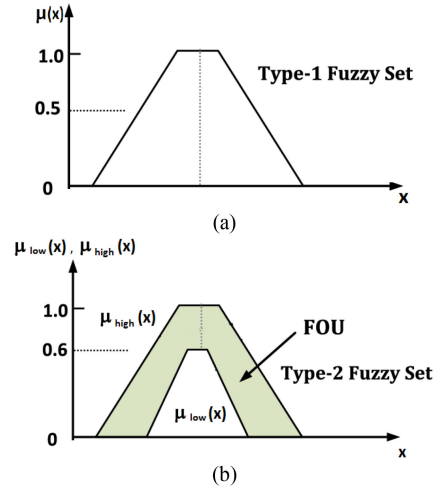


Fig. 1. Fuzzy membership function. (a) Type-1 fuzzy membership function. (b) Corresponding type-2 fuzzy membership function and FOU.

An interval type-2 fuzzy set is nothing but a fuzzy set with $\mu_S(x, v)=1$ and can be mathematically expressed as given in

$$\hat{S} = \{((x, v), 1) \mid \forall x \in X, \forall v \in J_x \subseteq [0, 1]\}. \quad (3)$$

Similarly, from (2), (4) can be derived by substituting $\mu_S(x, v)=1$

$$S = \int_{x \in X} \int_{v \in J_x} 1/(x, v), J_x \in [0, 1]. \quad (4)$$

The type-1 fuzzy membership function can be used to define interval type-2 fuzzy set as given as

$$\hat{S} = \left\{ \begin{array}{l} (x, \mu_{\text{low}}(x), \mu_{\text{high}}(x)) \mid \forall x \in X, \\ \mu_{\text{low}}(x) \leq \mu(x) \leq \mu_{\text{high}}(x), \mu \in [0, 1] \end{array} \right\} \quad (5)$$

where \hat{S} represents the interval type-2 fuzzy set, μ_x denotes the type-1 fuzzy membership, and $(\mu_{\text{low}}, \mu_{\text{high}})$ denotes the lower and upper membership of the interval type-2 fuzzy set and these can be obtained from type-1 fuzzy membership using (6) and (7), respectively. The interval type-2 fuzzy sets are basically the generalization of the interval-valued fuzzy sets [43]

$$\mu_{\text{low}} = [\mu(x)]^\lambda \quad (6)$$

$$\mu_{\text{high}} = [\mu(x)]^{1/\lambda}. \quad (7)$$

The parameter λ is known as the ‘‘fuzzy linguistic hedge,’’ and $\lambda \geq 1$. A fuzzy linguistic hedge can be considered as an operation that modifies the meaning of a fuzzy set. Fig. 1 shows a skeleton of the type-1 fuzzy membership function and its corresponding type-2 fuzzy membership function along with the footprint of uncertainty (FOU), i.e., the difference between upper and lower membership function.

B. Superpixel-Based Segmentation

Superpixel is a recently developed concept that is widely used for image segmentation purposes [44]. Superpixels are considered as a group of pixels that can be characterized by one or more

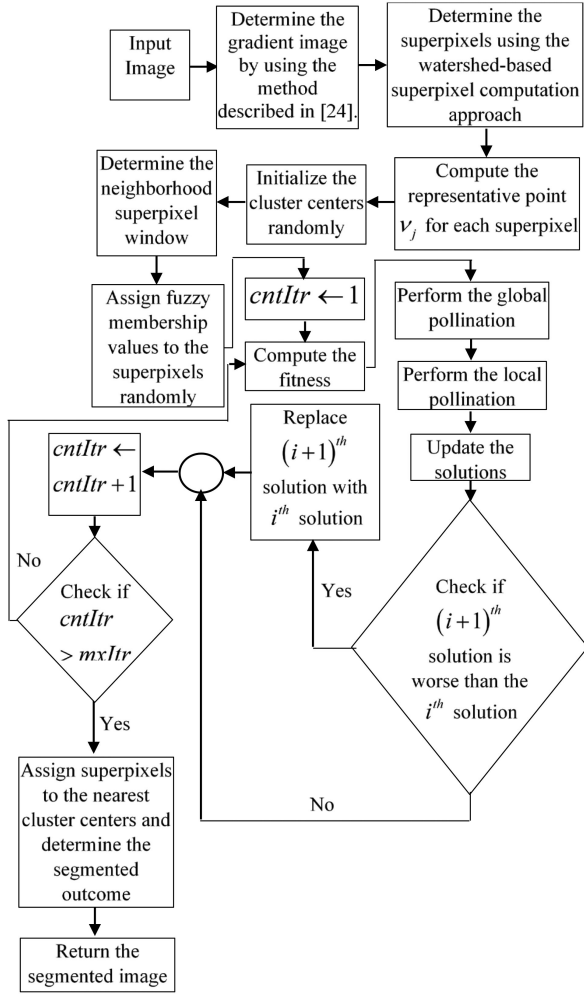


Fig. 2. Schematic flow diagram of the proposed approach.

than one similar characteristic. Superpixel segments an image based on visual characteristics with a very small amount of spatial information compared to the total amount of information available in an image. The count of the primitives is reduced with the help of superpixels that is highly beneficial in reducing the complexity in different tasks like pattern recognition, image classification, etc. One of the major advantages of using the concept of superpixel is that a meaningful delineated image can be obtained which is beneficial compared to pixel-based processing. The size and shape of the superpixels may vary depending on the method of superpixel computation. One of the most popular approaches known as simple linear iterative clustering [45] produces superpixels with regular regions. Two other approaches viz., watershed [46] and meanshift [47] generate irregular superpixels which are often useful in comparison to regular superpixels [48], [49]. The watershed-based approach to compute the superpixel is comparatively easier than the mean-shift approach. However, the watershed-based superpixel computation approach is sensitive to noise and is the main reason behind the popularity and widespread application of the mean-shift approach in finding superpixels of an image. Despite the noise sensitivity of the watershed-based approach, it is adopted

in the article owing to its simplicity. To reduce/eliminate the problem of noise sensitivity, the important edge information of the gradient image is preserved with the help of morphological opening and closing based reconstruction operations that are defined in (8) and (9), respectively. The important edge information is retrieved by finding the gradient image using the method described in [29]

$$\Phi_I^o(I') = \Phi_I^d(\Phi_I^e) \quad (8)$$

$$\Phi_I^e(I') = \Phi_I^e(\Phi_I^d) \quad (9)$$

where e and d denote the morphological erosion and dilation operation respectively and these operations are defined as

$$e_I^i(I') = e(e^{i-1}(I)) * I' \quad (10)$$

$$d_I^i(I') = d(d^{i-1}(I)) \circ I' \quad (11)$$

where “ $*$ ” and “ \circ ” denotes the point wise minimum and maximum value respectively while I and I' represent the actual and marker image, respectively. In the dilation operation, the value of the output pixels is computed by finding the maximum value among the neighborhood pixels. In the erosion operation, the value of the output pixels is computed by finding the minimum value among the neighborhood pixels. Equations (12) and (13) mathematically expresses the marker image I' , where E denotes the structuring element. The structuring element is used to probe the actual image I

$$I' = e_E(I) \quad (12)$$

$$I' = d_E(I). \quad (13)$$

Manual determination of structuring elements corresponding to different types of images may not always be feasible practically. Hence, different structuring elements are used to find the gradient images and amongst these images, point-wise maximum values are determined. The count of the structuring element is selected based on the range of the controlling parameter α where, $[\alpha_{low}, \alpha_{high}] \in \mathbb{N}^+$ and $\alpha_{low} \leq \alpha \leq \alpha_{high}$. Equation (14) is helpful in this purpose

$$\hat{\Phi}_I^O(I', \alpha_{low}, \alpha_{high}) = \max \left\{ \hat{\Phi}_I^O(I')_{E_{\alpha_{low}}}, \hat{\Phi}_I^O(I')_{E_{\alpha_{low}+1}}, \dots, \hat{\Phi}_I^O(I')_{E_{\alpha_{high}}} \right\}. \quad (14)$$

The upper limit can be computed with the help of an error controlling threshold ∂ and is defined as

$$\left\{ \hat{\Phi}_I^o(I', \alpha_{low}, \alpha_{high}) - \hat{\Phi}_I^o(I', \alpha_{low}, \alpha_{high} + 1) \right\} \leq \partial. \quad (15)$$

A group of pixels i.e., a superpixel j with total number of pixels cnt_j in the region R_j of the superpixel is represented by a representative value v_j , calculated using (16). From this equation, it can be noted that the arithmetic mean value is considered as the representative point of a superpixel

$$v_j = \frac{1}{cnt_j} \sum_{i \in R_j} \text{pixel}_i. \quad (16)$$

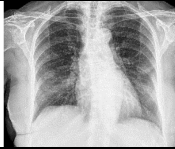
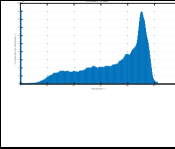
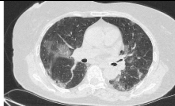
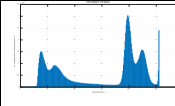

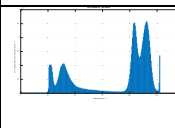

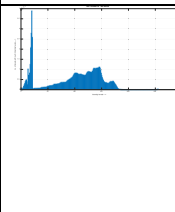
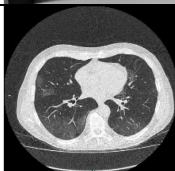
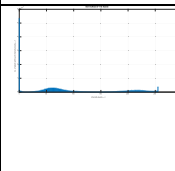
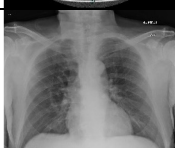
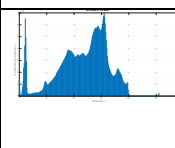
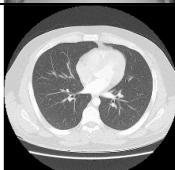
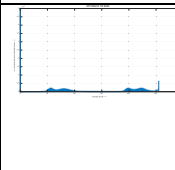

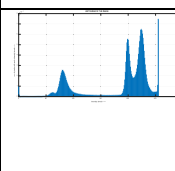
Id	View	Reference	Gender	Age	Modality	Image	Histogram	Remarks
I_1	Frontal	[59]	Female	70 years	X-Ray			Case courtesy of Dr Fabio Macori, Radiopaedia.org, rID: 74887 Bilateral ground-glass opacities are observed, COVID-19 pneumonia
I_2	Axial			CT				
I_3	Coronal			CT				
I_4	Lateral	[60]	Male	Not Known	X-Ray			Case courtesy of Dr Ali Mashalla Åhre, Radiopaedia.org, rID: 75037 mostly peripheral, opacifications can be observed, COVID-19 pneumonia
I_5	Axial	[61]	Male	75 years	CT			Case courtesy of Dr Domenico Nicoletti, Radiopaedia.org, rID: 75345 Large areas of ground glass opacities can be observed, COVID-19 pneumonia
I_6	Frontal			X-Ray				
I_7	Axial	[62]	Male	25 years	CT			Case courtesy of Dr Andrew Dixon, Radiopaedia.org, rID: 36676, CT scan of normal chest
I_8	Frontal							

Fig. 3. Description of the test images.

C. Interval Type-2 Fuzzy Clustering and Superpixel Based Segmentation

Typically, chest CT or X-Ray images contain a high correlation and therefore, a high dependency is observed among the pixels. Spatial interaction is sometimes essential to reduce the impact of noise. In this article, the advantages of superpixels are exploited and therefore, superpixels are considered as a unit instead of pixels. The concept of the superpixel-based local window that consists of a superpixel and its neighborhood is introduced in this article to incorporate spatial information in the segmentation process. So, increasing the size of the local window will incorporate more spatial information in the segmentation process. In this article, a 3×3 window size is considered.

The traditional objective function of the fuzzy c-means clustering algorithm is modified to incorporate the spatial information from the neighboring superpixel-based local window and is given as

$$\begin{aligned}
 J_{\phi}(x, y) = & \sum_{i=1}^c \sum_{j=1}^n (\mu'_{ij})^{\phi} \cdot \text{dist}_{ij}^2 \\
 & + \frac{\psi}{A_j} \sum_{i=1}^c \sum_{j=1}^n (\mu_{ij})^{\phi} \sum_{k \in NH_j} (\text{dist}_{ik})^2 \\
 & + \frac{\sigma}{A_j} \sum_{i=1}^c \sum_{j=1}^n (\mu_{ij})^{\phi} \sum_{k \in NH_j} (1 - \mu_{ik})^{\phi}. \quad (17)
 \end{aligned}$$



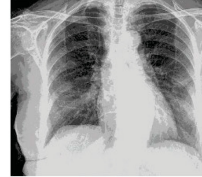


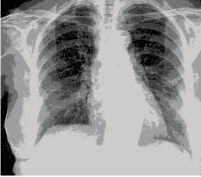
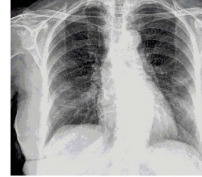
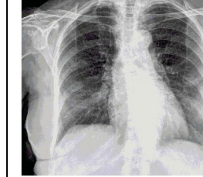





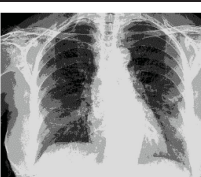
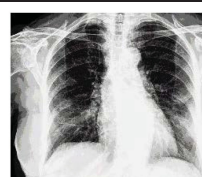
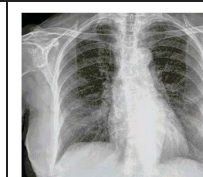


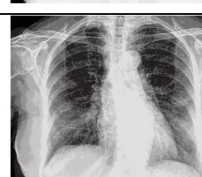
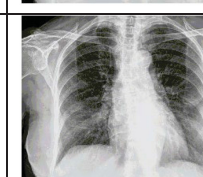
Algorithm	Number of Clusters			
	3	5	7	9
Black hole optimization [55]				
Modified cuckoo search [57]				
Fruit fly optimization [56]				
FEMO [58]				
Our proposed approach				

Fig. 4. Qualitative comparison of the segmented outcomes (image I_1 is used for this experiment).

In this equation, NH_j denotes the neighborhood of a superpixel S_j . A_j denotes the area of NH_j . dist_{ik} and μ_{ik} denote the distance and the membership, respectively, and these two terms are helpful to quantify the association of a superpixel to the cluster center. Here, ψ and σ are the weight coefficients that are used to control the impact of the compassionate term. One important point is that the conventional Euclidean distance measure may not always be useful in handling non-Euclidean input data. In this article, a non-Euclidean distance measure is adopted that is proposed in [50] where μ' and dist' are the modified membership and distance function, respectively. It can be noted that if we put $\psi=0, \sigma=0, \mu' = \mu, \text{dist}' = \text{dist}$, then this approach converges to the traditional fuzzy c-means clustering approach. This approach is designed to get applied to the superpixels, hence, the representative value of a superpixel is used to incorporate the spatial information. In the conventional fuzzy c-means clustering approach, the association of a superpixel S_j to the cluster i depends on the membership value μ_{ij} . But, the spatial information that is provided by the superpixel-based spatial window cannot be considered while determining the membership unless the membership function

is modified appropriately. To solve this issue, the conventional membership function is modified to incorporate the information from the superpixel-based neighboring window and presented as

$$\mu_{ij}^{\text{SupSpatial}} = \sum_{k \in NH_j} \mu_{ik} \cdot \mu_{kj}. \quad (18)$$

In this equation, μ_{ik} denotes traditional fuzzy membership of a superpixel S_j to the i^{th} cluster center. The second term,

i.e., μ_{kj} is incorporated to model the connection between a superpixel S_j and its neighborhood S_k and it can be observed that the value of it must be inversely proportional to the distance between the superpixel S_j and its neighborhood S_k . So, it can be expressed as given as

$$\mu_{kj} = \frac{1}{\sum_{t=1}^{NH_j} \left(\frac{\text{dist}^2(s_k, s_j)}{\text{dist}^2(s_t, s_j)} \right)^{\frac{1}{\phi-1}}}. \quad (19)$$

TABLE I
AVERAGE QUANTITATIVE RESULTS FOR DIFFERENT VALIDITY INDICES AND DIFFERENT NUMBER OF CLUSTERS (ACCEPTABLE VALUES ARE HIGHLIGHTED IN THE BOLDFACE)

Validity Indices	Algorithm	No. of Clusters			
		3	5	7	9
Davies–Bouldin index	Black hole optimization [55]	1.974805	1.578876	2.020856	0.790946
	Modified cuckoo search [57]	0.977695	2.201828	2.996354	2.330085
	Fruit fly optimization [56]	1.380057	1.571357	1.526752	2.26197
	FEMO [58]	1.874774	2.103211	1.159496	2.274487
	Proposed approach	1.443608	1.176849	0.775509	1.7979
Xie-Beni index	Black hole optimization [55]	2.791858	3.550655	2.889839	2.72089
	Modified cuckoo search [57]	2.24271	2.391077	1.473192	1.989232
	Fruit fly optimization [56]	1.902956	4.19241	3.869503	2.866116
	FEMO [58]	3.236071	2.237116	2.436067	3.162285
	Proposed approach	2.011178	1.35928	1.414806	1.909993
Dunn index	Black hole optimization [55]	1.373943069	1.550163993	3.781000893	1.431586525
	Modified cuckoo search [57]	4.561908072	4.360595816	4.332799673	2.426414294
	Fruit fly optimization [56]	4.184614121	2.505749356	3.007967629	2.716099326
	FEMO [58]	3.253360176	3.586293011	2.840439657	4.52583222
	Proposed approach	1.769690993	4.665662343	1.49183224	1.510382413
β index	Black hole optimization [55]	1.213357326	3.013975908	3.345945018	1.987814638
	Modified cuckoo search [57]	0.562751793	0.627912078	3.249229689	3.072608845
	Fruit fly optimization [56]	0.756777167	0.375754365	1.735223997	2.164460594
	FEMO [58]	3.717977224	1.335898738	1.879328264	1.718581677
	Proposed approach	0.330262509	2.540809403	3.300655431	2.146909293

By substituting the value of (16) into (19), we get

$$\mu_{kj} = \frac{1}{\sum_{t=1}^{NH_j} \left(\frac{\text{dist}^2 \left(\frac{1}{\text{cnt}_k} \sum_{i \in R_k} \text{pixel}_i, \frac{1}{\text{cnt}_j} \sum_{i \in R_j} \text{pixel}_i \right)}{\text{dist}^2 \left(\frac{1}{\text{cnt}_t} \sum_{i \in R_t} \text{pixel}_i, \frac{1}{\text{cnt}_j} \sum_{i \in R_j} \text{pixel}_i \right)} \right)^{\frac{1}{\phi-1}}}. \quad (20)$$

By substituting the value of (20) into (18), we get (21) as follows:

$$\begin{aligned} \mu_{ij}^{\text{SupSpatial}} &= \sum_{k \in NH_j} \mu_{ik} \\ &= \sum_{t=1}^{NH_j} \left(\frac{\text{dist}^2 \left(\frac{1}{\text{cnt}_k} \sum_{i \in R_k} \text{pixel}_i, \frac{1}{\text{cnt}_j} \sum_{i \in R_j} \text{pixel}_i \right)}{\text{dist}^2 \left(\frac{1}{\text{cnt}_t} \sum_{i \in R_t} \text{pixel}_i, \frac{1}{\text{cnt}_j} \sum_{i \in R_j} \text{pixel}_i \right)} \right)^{-\frac{1}{\phi-1}} \\ &= \sum_{t=1}^{NH_j} \left(\frac{1}{\text{dist}^2 \left(\frac{1}{\text{cnt}_t} \sum_{i \in R_t} \text{pixel}_i, \frac{1}{\text{cnt}_j} \sum_{i \in R_j} \text{pixel}_i \right)} \right)^{-\frac{1}{\phi-1}} \\ &= \sum_{k=1}^{NH_j} \left(\frac{\mu_{ik}}{\text{dist}^2 \left(\frac{1}{\text{cnt}_t} \sum_{i \in R_t} \text{pixel}_i, \frac{1}{\text{cnt}_j} \sum_{i \in R_j} \text{pixel}_i \right)^{\frac{1}{\phi-1}}} \right). \quad (21) \end{aligned}$$

This membership function is used to incorporate the neighborhood details of the superpixel and also helpful to exploit the advantages of the superpixel. In this article, the cluster centers are updated with the help of the enhanced flower pollination algorithm [38].

This approach is applied in segmenting chest CT and X-Ray images that are helpful for the physicians by acting as a third eye in detecting the COVID-19 infection quickly and precisely. The proposed algorithm is illustrated in Algorithm 1 and the schematic flow diagram of the proposed approach is depicted in Fig. 2.

III. EXPERIMENTAL RESULTS AND ANALYSIS

A. Dataset Description

The proposed approach is applied and evaluated on 300 chest CT scan images as well as 250 X-Ray images that are collected from some publicly available web repositories like Radiopaedia.org, sirm.org, figshare, kaggle. Typically, it is always preferable to compare the outcome of an unsupervised classification approach with some ground truth images. But, one of the main inspirations to design this approach is the non-availability of the ground truth data. Practically, it is very hard to obtain a manually delineated dataset that is performed by some domain experts. Hence, four standard cluster validity indices, such as Davies–Bouldin (DB) index [51], Xie-Beni (XB) index [52], Dunn index [53], and β index [54] are used to quantify the experimental outcome. Amongst all images, segmentation outcomes of 8 images are reported in this article and the details of these images are given in Fig. 3. From the description of Fig. 3, it is

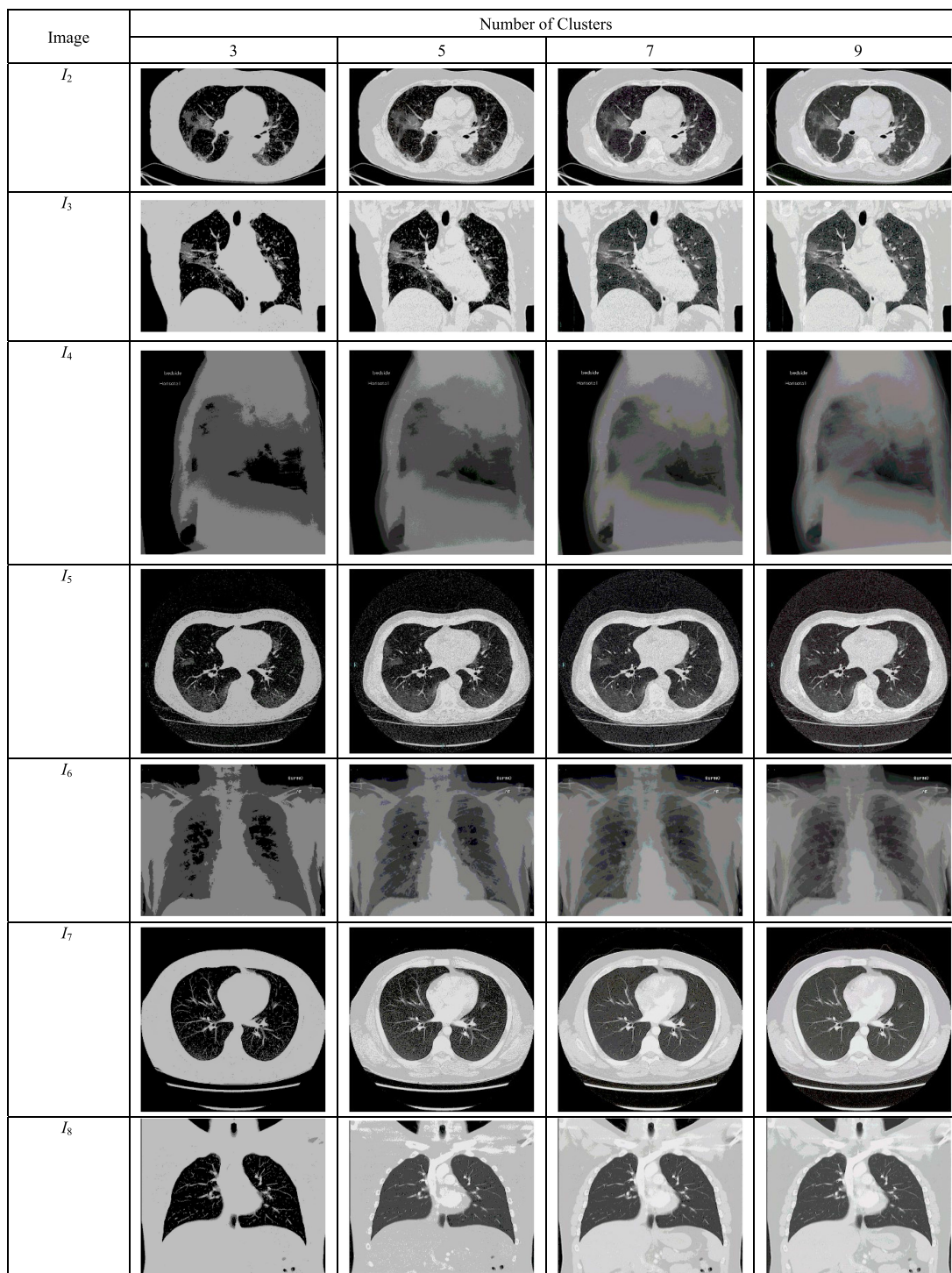


Fig. 5. Segmented outcomes obtained after applying the proposed approach.

observed that both normal cases and COVID-19 infected cases are considered for the investigation purposes.

B. Experimental Results

Experiments are carried out in MATLAB R2020a environment that is installed on a computer well equipped with Intel Core i3 processor (1.8 GHz), 4 GB RAM, and 500 GB HDD.

Both qualitative and quantitative analysis is carried out to test the performance of the proposed approach.

The proposed approach is compared with some state-of-the-art techniques such as black hole optimization (BHO) [55], fruit fly optimization (FFO) [56], modified cuckoo search (MCS) [57], and fuzzy electromagnetism optimization (FEMO) [58]. It is noted that this approach does not use any training dataset or ground truth data, and therefore, it is not possible to compare

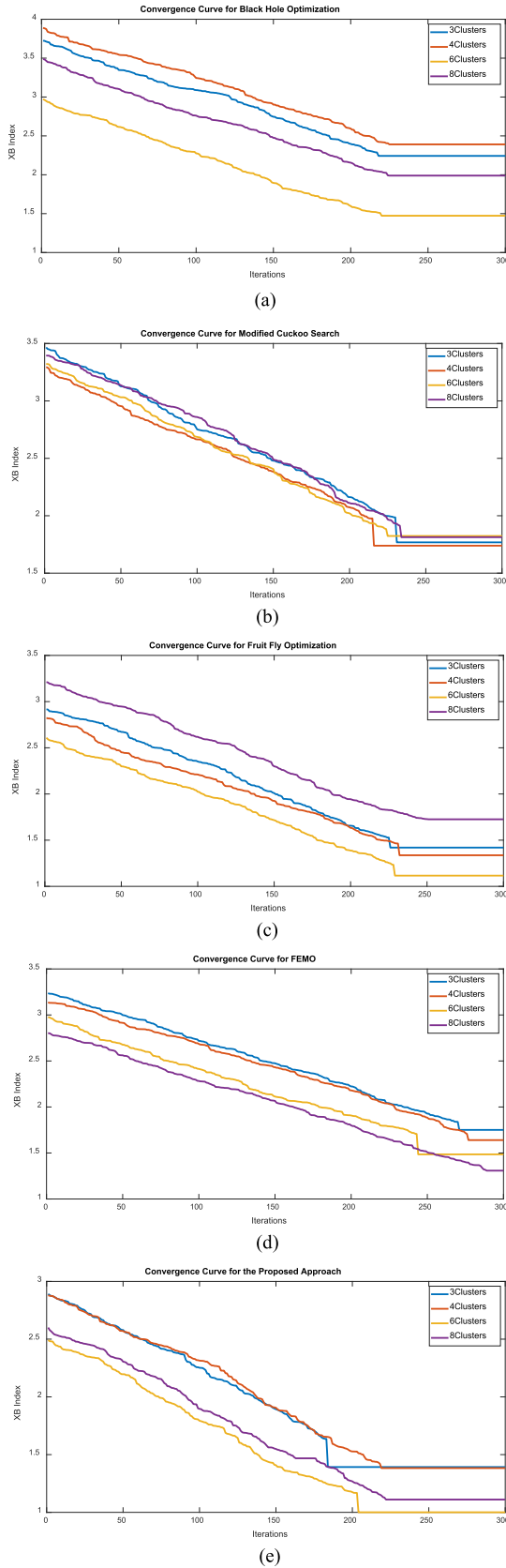


Fig. 6. Graphical comparison of the convergence. (a) Black hole optimization [55]. (b) Modified Cuckoo search [57]. (c) Fruit fly optimization [56]. (d) FEMO [58]. (e) Proposed approach. In X-axis, the number of iterations and in Y-axis, the value of the Xie-Beni index are plotted.

Algorithm 1: The proposed approach

Input: Image for segmentation

Output: Output image for segmentation

- 1: Determine the gradient image by using the method described in [29].
 - 2: Determine the superpixels using the watershed-based superpixel computation approach as described in subsection II.B.
 - 3: Compute the representative point v_j for each superpixel.
 - 4: Initialize the cluster centers randomly using $CEN_k = \nu_{low} + \text{rand}(0, 1) \cdot (\nu_{high} - \nu_{low})$. The lower and upper bound of a representative point for a superpixel is denoted with ν_{low} and ν_{high} respectively.
 - 5: Determine the neighborhood superpixel window.
 - 6: Assign fuzzy membership values to the superpixels randomly.
 - 7: $cntItr \leftarrow 1$ //iteration counter
 - 8: Repeat until $(cntItr > mxItr)$ // $mxItr$ is the maximum number of iterations
 - 9: Compute the fitness
 - 10: Perform the global pollination
 - 11: Perform the local pollination
 - 12: Update the solutions
 - 13: Check if $(i + 1)^{th}$ solution is worse than the i^{th} solution then
 - 14: Replace $(i + 1)^{th}$ solution with i^{th} solution. End if
 - 15: Update the global best
 - 16: $cntItr \leftarrow cntItr + 1$ end until
 - 17: Assign superpixels to the nearest cluster centers and determine the segmented outcome.
 - 18: Return the segmented image.
-

with some supervised approaches. The comparative qualitative results for the image I_1 are reported in Fig. 4 and the segmentation results (obtained after applying the proposed approach) for the rest of the seven images are reported in Fig. 5.

It is observed that the experiments are carried out for the different number of clusters. For the sake of conciseness, the authors have avoided representing the values of different indices for each image. Instead of that, the average values of different indices for the different numbers of clusters are given in Table I. Fig. 7 illustrates the obtained results graphically with the help of heat maps. The results are illustrated for different cluster validity indices. For every index i.e., DB index, XB index, Dunn index, and β index a separate figure is incorporated that helps in the easy interpretation of the results.

C. Analysis of Convergence Rate

The analysis of the rate of convergence is one of the very important aspects that are to be explored and analyzed properly. In this section, a comparative overview of different approaches with a different number of clusters is reported with a graphical representation. Fig. 7 shows five different images for five algorithms under consideration where the number of iterations is

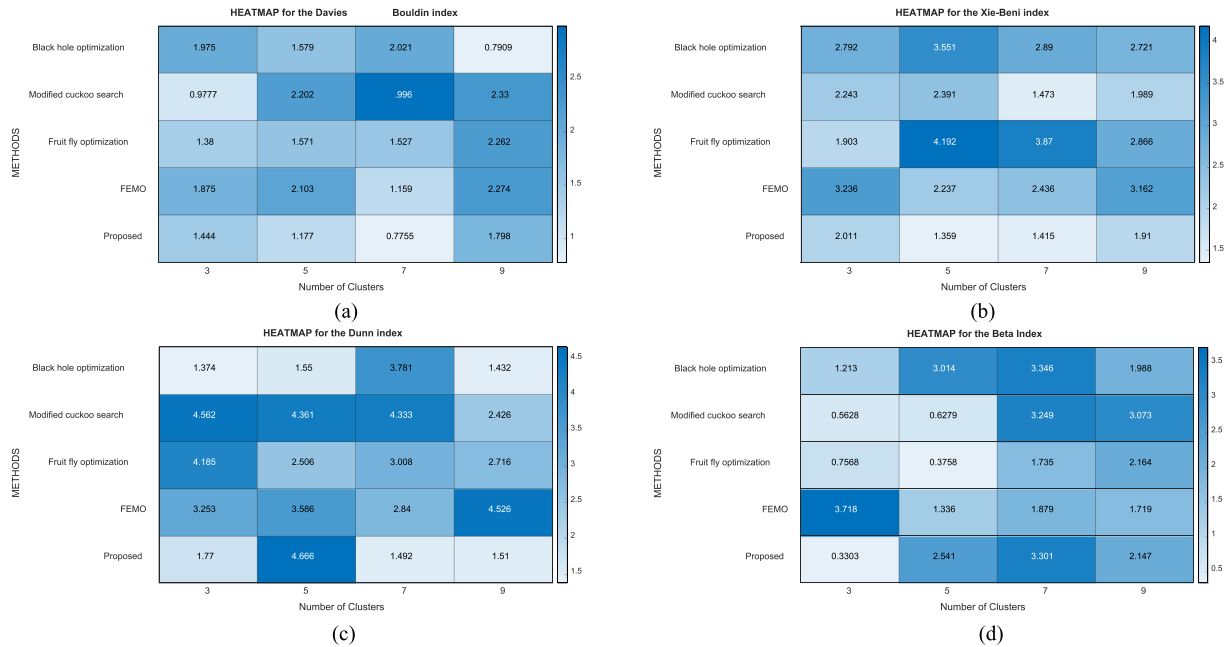


Fig. 7. Graphical comparison (heatmap based) of the obtained results corresponding to the (a) DB Index, (b) XB index, (c) Dunn index, and (d) β index.

plotted in X -axis and the value of the Xie-Beni index is plotted in Y -axis. In each image, four lines indicate the convergence of four clusters. From Fig. 5, it is observed that the proposed approach outperforms other approaches in terms of convergence. It is achieved by reducing the computational burden by incorporating the concept of the superpixel. Moreover, it can also be noted that the proposed approach works well for a higher number of clusters that are significant for the real-life deployment of the proposed approach.

IV. DISCUSSION

The proposed approach is an unsupervised means of diagnosing the COVID-19 infection from the chest radiological images. The main advantage of this approach is that it does not depend on manual delineations and can work without explicitly being trained. Moreover, the cluster centers can be randomly selected, and that there is no need to choose the cluster centers manually. The fact that the proposed approach reduces computational overhead is reflected in the convergence curves.

It can be observed that the proposed approach works well for the higher number of clusters. However, the method cannot determine the number of clusters automatically which is certainly a problem. Although the proposed approach can be used as an additional tool for early and easy diagnosis of the COVID-19 infection from radiological images, however, it cannot clearly differentiate between COVID-19 and other infections owing to the non-availability of training data and hence can only highlight the infected regions leaving the final diagnosis for the physicians and other domain experts. Hence, the manual diagnosis seems to be another limitation of the proposed approach.

In Table I, average quantitative results for different validity indices and the different number of clusters are presented and the

acceptable values are highlighted in the boldface. From the earlier discussion, it can be understood that the proposed approach cannot determine an optimal number of clusters depending on the test image. It can be considered a limitation of the proposed work and interesting future work.

Four different cluster validity indices are used for evaluation purposes. Out of these four indices, Davies–Bouldin index, and Xie-Beni index are expected to be minimized whereas the Dunn index, and β index is expected to be maximized. Validation indices measure compactness, connectedness, and separation and can be chosen based on the cluster types and the underlying algorithm. This approach compares four well-known validity indices to prove the effectiveness of the proposed approach.

The highlighted values represent the best value obtained by a certain method and the corresponding number of clusters can be considered the optimal number of clusters determined by that approach. However, a certain number of clusters that is determined as the optimal number of clusters by an approach does not need to be the same as the optimal number of clusters that is determined by another approach. Hence, to interpret this table, it is necessary to compare the best values obtained by each approach because column-wise comparison may lead to ambiguity. So, from Table I, it can be observed that the proposed approach outperforms other state-of-the-art approaches in most the scenarios (except for β index where the proposed approach is marginally outperformed by the BHO and FEMO).

V. CONCLUSION

The proposed approach is designed to help the physicians and other domain experts to some extent so that the early identification and screening process gets easier. The experimental outcomes also support the fact that the proposed approach

can be deployed in various real-life scenarios that can help in better management of this pandemic scenario. One of the major advantages of this approach is the nondependency on the manual or experts' delineations. Moreover, this approach is not dependent on the choice of the initial cluster centers. The experimental outcomes establish that the proposed approach outperforms some of the state-of-the-art approaches in terms of both qualitatively and quantitatively.

One major drawback of the proposed approach is the dependency on the cluster count i.e., this approach cannot determine the number of clusters automatically. It is to be incorporated in our future works to make this approach more realistic and suitable for real-life applications. The proposed approach also be evaluated with some other validity measures and further investigations can be made to improve the proposed approach. The proposed work also gives satisfactory results in terms of convergence and also outperforms some of the standard approaches. At last, it should be carefully noted that neither the proposed approach can be considered as a gold standard for detection of COVID-19 disease nor it can replace some standard COVID-19 infection detection measures like the RT-PCR test. This approach will certainly be beneficial to diagnose the COVID-19 infection by acting as a third eye for the domain experts that will certainly accelerate the supportive treatment process initiation of the safety protocols.

ACKNOWLEDGMENT

The authors would like to express their gratitude and thank the editors, anonymous reviewers, and referees for their valuable comments and suggestions, which are helpful in further improvement of this article.

REFERENCES

- [1] G. Chassagnon *et al.*, "AI-driven quantification, staging and outcome prediction of COVID-19 pneumonia," *Med. Image Anal.*, vol. 67, Jan. 2021, Art. no. 101860.
- [2] X. Wu, C. Chen, M. Zhong, J. Wang, and J. Shi, "COVID-AL: The diagnosis of COVID-19 with deep active learning," *Med. Image Anal.*, vol. 68, Feb. 2021, Art. no. 101913.
- [3] S. Bhattacharya *et al.*, "Deep learning and medical image processing for coronavirus (COVID-19) pandemic: A survey," *Sustain. Cities Soc.*, vol. 65, Feb. 2021, Art. no. 102589.
- [4] M. A. Khan *et al.*, "Prediction of COVID-19 - Pneumonia based on selected deep features and one class kernel extreme learning machine," *Comput. Elect. Eng.*, vol. 90, Mar. 2021, Art. no. 106960.
- [5] Y. Oh, S. Park, and J. C. Ye, "Deep learning COVID-19 features on CXR using limited training data sets," *IEEE Trans. Med. Imag.*, vol. 39, no. 8, pp. 2688–2700, May 2020.
- [6] S. Roy *et al.*, "Deep learning for classification and localization of COVID-19 markers in Point-of-Care lung ultrasound," *IEEE Trans. Med. Imag.*, vol. 39, no. 8, pp. 2676–2687, Aug. 2020.
- [7] J. Civit-Masot, F. Luna-Perejón, M. D. Morales, and A. Civit, "Deep learning system for COVID-19 diagnosis aid using X-ray pulmonary images," *Appl. Sci.*, vol. 10, no. 13, Jul. 2020, Art. no. 4640.
- [8] C. Butt, J. Gill, D. Chun, and B. A. Babu, "Deep learning system to screen coronavirus disease 2019 pneumonia," *Appl. Intell.*, 2020. [Online]. Available: <https://doi.org/10.1007/s10489-020-01714-3>
- [9] S. Wang *et al.*, "A deep learning algorithm using CT images to screen for corona virus disease (COVID-19)," *medRxiv*, Apr. 2020. [Online]. Available: <https://doi.org/10.1101/2020.02.14.20023028>
- [10] X. Xu *et al.*, "Deep learning system to screen coronavirus disease 2019 pneumonia," Mar. 2020. Accessed: Mar. 27, 2020. [Online]. Available: arxiv.org/abs/2002.09334
- [11] J. Chen, K. Li, Z. Zhang, K. Li, and P. S. Yu, "A survey on applications of artificial intelligence in fighting against COVID-19," Jul. 2020. Accessed: Jul. 15, 2020. [Online]. Available: arxiv.org/abs/2007.02202
- [12] H. Chao *et al.*, "Integrative analysis for COVID-19 patient outcome prediction," *Med. Image Anal.*, vol. 67, Jan. 2021, Art. no. 101844.
- [13] K. Gao *et al.*, "Dual-branch combination network (DCN): Towards accurate diagnosis and lesion segmentation of COVID-19 using CT images," *Med. Image Anal.*, vol. 67, Jan. 2021, Art. no. 101836.
- [14] S. Minaee, R. Kafieh, M. Sonka, S. Yazdani, and G. J. Soufi, "Deep-COVID: Predicting COVID-19 from chest X-Ray images using deep transfer learning," *Med. Image Anal.*, vol. 65, Apr. 2020, Art. no. 101794. Accessed: Jul. 26, 2020. [Online]. Available: arxiv.org/abs/2004.09363
- [15] S. Chakraborty and K. Mali, "An overview of biomedical image analysis from the deep learning perspective," in *Applications of Advanced Machine Intelligence in Computer Vision and Object Recognition: Emerging Research and Opportunities*, S. Chakraborty and K. Mali, Eds., Hershey, PA, USA: IGI Global, 2020.
- [16] S. Chakraborty, S. Chatterjee, A. S. Ashour, K. Mali, and N. Dey, "Intelligent computing in medical imaging: A study," in *Advancements in Applied Metaheuristic Computing*, N. Dey, Ed., Hershey, PA, USA: IGI Global, 2017, pp. 143–163.
- [17] A. Amyar, R. Modzelewski, H. Li, and S. Ruan, "Multi-task deep learning based CT imaging analysis for COVID-19 pneumonia: Classification and segmentation," *Comput. Biol. Med.*, vol. 126, Nov. 2020, Art. no. 104037.
- [18] P. L. Vidal, J. de Moura, J. Novo, and M. Ortega, "Multi-stage transfer learning for lung segmentation using portable X-ray devices for patients with COVID-19," *Expert Syst. Appl.*, vol. 173, Jul. 2021, Art. no. 114677.
- [19] S. El-bana, A. Al-Kabbany, and M. Sharkas, "A multi-task pipeline with specialized streams for classification and segmentation of infection manifestations in COVID-19 scans," *PeerJ Comput. Sci.*, vol. 6, Oct. 2020, Art. no. e303.
- [20] M. Blain *et al.*, "Determination of disease severity in COVID-19 patients using deep learning in chest X-ray images," *Diagn. Interventional Radiol.*, vol. 27, no. 1, pp. 20–27, Jan. 2021.
- [21] D.-P. Fan *et al.*, "Inf-Net: Automatic COVID-19 lung infection segmentation from CT images," *IEEE Trans. Med. Imag.*, vol. 39, no. 8, pp. 2626–2637, Aug. 2020.
- [22] T. Zheng *et al.*, "Unsupervised segmentation of COVID-19 infected lung clinical CT volumes using image inpainting and representation learning," in *Proc. Med. Imag., Image Process.*, Feb. 2021, vol. 11596, [Online]. Available: <https://doi.org/10.1117/12.2580641>
- [23] S. Chakraborty and K. Mali, "SUFMACS: A machine learning-based robust image segmentation framework for covid-19 radiological image interpretation," *Expert Syst. Appl.*, vol. 1758, Apr. 2021, Art. no. 115069.
- [24] S. Chakraborty and K. Mali, "A morphology-based radiological image segmentation approach for efficient screening of COVID-19," *Biomed. Signal Process. Control*, vol. 69, May 2021, Art. no. 102800.
- [25] F. Shi *et al.*, "Review of artificial intelligence techniques in imaging data acquisition, segmentation, and diagnosis for COVID-19," *IEEE Rev. Biomed. Eng.*, vol. 14, pp. 4–15, Apr. 2021.
- [26] A. Ulhaq, A. Khan, D. Gomes, and M. Paul, "Computer vision for COVID-19 control: A survey," Apr. 2020. Accessed: Jul. 15, 2020. [Online]. Available: arxiv.org/abs/2004.09420
- [27] E. Tartaglione, C. A. Barbano, C. Berzovini, M. Calandri, and M. Grangetto, "Unveiling COVID-19 from CHEST X-Ray with deep learning: A hurdles race with small data," *Int. J. Environ. Res. Public Health*, vol. 17, no. 18, Sep. 2020, Art. no. 6933.
- [28] A. Ulhaq, J. Born, A. Khan, D. P. S. Gomes, S. Chakraborty, and M. Paul, "COVID-19 control by computer vision approaches: A survey," *IEEE Access*, vol. 8, pp. 179437–179456, Sep. 2020.
- [29] S. Hore *et al.*, "Finding contours of hippocampus brain cell using microscopic image analysis," *J. Adv. Microsc. Res.*, vol. 10, no. 2, pp. 93–103, Jun. 2015.
- [30] S. Hore *et al.*, "An integrated interactive technique for image segmentation using stack based seeded region growing and thresholding," *Int. J. Elect. Comput. Eng.*, vol. 6, no. 6, pp. 2773–2780, Oct. 2016.
- [31] S. Chakraborty, K. Mali, A. Banerjee, and M. Bhattacharjee, "A biomedical image segmentation approach using fractional order darwinian particle swarm optimization and thresholding," in *Advances in Smart Communication Technology and Information Processing*, Singapore: Springer, 2021, pp. 299–306.
- [32] S. Chakraborty, "An advanced approach to detect edges of digital images for image segmentation," in *Applications of Advanced Machine Intelligence in Computer Vision and Object Recognition: Emerging Research and Opportunities*, S. Chakraborty and K. Mali, Eds., Hershey, PA, USA: IGI Global, 2020.

- [33] X. Wang *et al.*, "A weakly-supervised framework for COVID-19 classification and lesion localization from chest cT," *IEEE Trans. Med. Imag.*, vol. 39, no. 8, pp. 2615–2625, Aug. 2020.
- [34] S. Chakraborty and K. Mali, "Application of multiobjective optimization techniques in biomedical image Segmentation—A study," in *Multi-Objective Optimization*, Singapore: Springer, 2018, pp. 181–194.
- [35] K. Mittal, A. Jain, K. S. Vaisla, O. Castillo, and J. Kacprzyk, "A comprehensive review on type 2 fuzzy logic applications: Past, present, and future," *Eng. Appl. Artif. Intell.*, vol. 95, Oct. 2020, Art. no. 103916.
- [36] Q. Liang and J. M. Mendel, "Equalization of nonlinear time-varying channels using type-2 fuzzy adaptive filters," *IEEE Trans. Fuzzy Syst.*, vol. 8, no. 5, pp. 551–563, Oct. 2000.
- [37] H. R. Tizhoosh, "Image thresholding using type II fuzzy sets," *Pattern Recognit.*, vol. 38, no. 12, pp. 2363–2372, Dec. 2005.
- [38] S. T. Mohamed, H. M. Ebeid, A. E. Hassanien, and M. F. Tolba, "A hybrid flower pollination optimization based modified multi-scale retinex for blood cell microscopic image enhancement," in *Proc. 3rd IEEE Int. Conf. Res. Comput. Intell. Commun. Netw.*, Dec. 2017, vol. 2017, pp. 225–230.
- [39] X. S. Yang, "Flower pollination algorithm for global optimization," in *Lecture Notes in Computer Science (including subseries Lecture Notes in Artificial Intelligence and Lecture Notes in Bioinformatics)*, vol. 7445 LNCS, New York, NY, USA: Springer, 2012, .
- [40] M. Abdel-Basset and L. A. Shawky, "Flower pollination algorithm: A comprehensive review," *Artif. Intell. Rev.*, vol. 52, no. 4, pp. 2533–2557, Dec. 2019.
- [41] S. Chakraborty and S. Bhowmik, "An efficient approach to job shop scheduling problem using simulated annealing," *Int. J. Hybrid Inf. Technol.*, vol. 8, no. 11, pp. 273–284, 2015.
- [42] J. M. Mendel and R. I. B. John, "Type-2 fuzzy sets made simple," *IEEE Trans. Fuzzy Syst.*, vol. 10, no. 2, pp. 117–127, Apr. 2002.
- [43] H. B. Sola, J. Fernandez, H. Hagra, F. Herrera, M. Pagola, and E. Barrenechea, "Interval type-2 fuzzy sets are generalization of interval-valued fuzzy sets: Toward a wider view on their relationship," *IEEE Trans. Fuzzy Syst.*, vol. 23, no. 5, pp. 1876–1882, Oct. 2015.
- [44] S. Chakraborty and K. Mali, "SuFMoFPA: A superpixel and meta-heuristic based fuzzy image segmentation approach to explicate COVID-19 radiological images," *Expert Syst. Appl.*, vol. 167, Oct. 2020, Art. no. 114142.
- [45] R. Achanta, A. Shaji, K. Smith, A. Lucchi, P. Fua, and S. Süsstrunk, "SLIC superpixels compared to state-of-the-art superpixel methods," *IEEE Trans. Pattern Anal. Mach. Intell.*, vol. 34, no. 11, pp. 2274–2281, Nov. 2012.
- [46] Z. Hu, Q. Zou, and Q. Li, "Watershed superpixel," in *Proc. Int. Conf. Image Process.*, Dec. 2015, pp. 349–353.
- [47] D. Comaniciu and P. Meer, "Mean shift: A robust approach toward feature space analysis," *IEEE Trans. Pattern Anal. Mach. Intell.*, vol. 24, no. 5, pp. 603–619, May 2002.
- [48] T. Lei, X. Jia, Y. Zhang, S. Liu, H. Meng, and A. K. Nandi, "Superpixel-Based fast fuzzy C-Means clustering for color image segmentation," *IEEE Trans. Fuzzy Syst.*, vol. 27, no. 9, pp. 1753–1766, Sep. 2019.
- [49] Y. Guo, L. Jiao, S. Wang, S. Wang, F. Liu, and W. Hua, "Fuzzy superpixels for polarimetric SAR images classification," *IEEE Trans. Fuzzy Syst.*, vol. 26, no. 5, pp. 2846–2860, Oct. 2018.
- [50] D. Q. Zhang and S. C. Chen, "A novel kernelized fuzzy C-means algorithm with application in medical image segmentation," *Artif. Intell. Med.*, vol. 32, no. 1, pp. 37–50, Sep. 2004.
- [51] D. L. Davies and D. W. Bouldin, "A cluster separation measure," *IEEE Trans. Pattern Anal. Mach. Intell.*, vol. PAMI-1, no. 2, pp. 224–227, Apr. 1979.
- [52] X. L. Xie and G. Beni, "A validity measure for fuzzy clustering," *IEEE Trans. Pattern Anal. Mach. Intell.*, vol. 13, no. 8, pp. 841–847, Aug. 1991.
- [53] J. C. Dunn, "Well-separated clusters and optimal fuzzy partitions," *J. Cybern.*, vol. 4, no. 1, pp. 95–104, 1974.
- [54] S. K. Pal, A. Ghosh, and B. U. Shankar, "Segmentation of remotely sensed images with fuzzy thresholding, and quantitative evaluation," *Int. J. Remote Sens.*, vol. 21, no. 11, pp. 2269–2300, 2000.
- [55] P. Upadhyay, "Brain MRI image segmentation using nature-inspired black hole metaheuristic clustering approach," in *Computational Intelligence and its Applications in Healthcare*, Amsterdam, The Netherlands: Elsevier, 2020, pp. 37–51.
- [56] H. Zhu, H. He, J. Xu, Q. Fang, and W. Wang, "Medical image segmentation using fruit fly optimization and density peaks clustering," *Comput. Math. Methods Med.*, vol. 2018, 2018, Art. no. 3052852.
- [57] S. Chakraborty *et al.*, "Modified cuckoo search algorithm in microscopic image segmentation of hippocampus," *Microsc. Res. Tech.*, vol. 80, no. 10, pp. 1051–1072, Oct. 2017.
- [58] S. Chakraborty and K. Mali, "Fuzzy electromagnetism optimization (FEMO) and its application in biomedical image segmentation," *Appl. Soft Comput.*, vol. 97, Dec. 2020, Art. no. 106800.
- [59] "COVID-19 pneumonia | radiology case | Radiopaedia.org." Accessed: May 6, 2020. [Online]. Available: <https://radiopaedia.org/cases/covid-19-pneumonia-14>
- [60] "COVID-19 pneumonia | radiology case | Radiopaedia.org." Accessed: Feb. 28, 2021. [Online]. Available: <https://radiopaedia.org/cases/covid-19-pneumonia-15>
- [61] "COVID-19 pneumonia | radiology case | Radiopaedia.org." Accessed: Mar. 21, 2021. [Online]. Available: <https://radiopaedia.org/cases/covid-19-pneumonia-35>
- [62] "Normal CT chest | radiology case | radiopaedia.org." Accessed: Mar. 5, 2021. [Online]. Available: <https://radiopaedia.org/cases/normal-ct-chest>



Weiping Ding (Senior Member, IEEE) received the Ph.D. degree in computer science from the Nanjing University of Aeronautics and Astronautics, Nanjing, China, in 2013.

He was a Visiting Scholar with the University of Lethbridge, Lethbridge, AB, Canada, in 2011. From 2014 to 2015, he was a Postdoctoral Researcher with the Brain Research Center, National Chiao Tung University, Hsinchu, Taiwan. In 2016, he was a Visiting Scholar with the National University of Singapore, Singapore. From 2017 to 2018, he was a Visiting

Professor with the University of Technology Sydney, Ultimo, NSW, Australia. He has authored or coauthored more than 100 research peer-reviewed journal and conference papers, including *IEEE TRANSACTIONS ON FUZZY SYSTEMS*, *IEEE TRANSACTIONS ON NEURAL NETWORKS AND LEARNING SYSTEMS*, *IEEE TRANSACTIONS ON CYBERNETICS*, *IEEE SYSTEMS, MAN, AND CYBERNETICS*, *IEEE TRANSACTIONS ON BIOMEDICAL ENGINEERING*, *IEEE TRANSACTIONS ON INDUSTRIAL INFORMATICS*, *IEEE TRANSACTIONS ON EMERGING TOPICS IN COMPUTATIONAL INTELLIGENCE*, and *IEEE TRANSACTIONS ON INTELLIGENT TRANSPORTATION SYSTEMS*, etc. His main research directions involve deep neural networks, multimodal machine learning, granular data mining, uncertainty modeling in big data, coevolutionary algorithm, and medical images analysis.

Dr. Ding is the Chair of IEEE CIS Task Force on Granular Data Mining for Big Data. He is a Member IEEE Computational Intelligence Society, *Association for Computing Machinery*, CCAI, and Senior CCF. He is a member of Technical Committee on Soft Computing of IEEE SMCS, on Granular Computing of IEEE SMCS, and on Data Mining and Big Data Analytics of IEEE CIS. He is currently serving on the Editorial Advisory Board of *Knowledge-Based Systems* and Editorial Board of *Information Fusion*, *Applied Soft Computing*, and *Neurocomputing*. He is/was an Associate Editor for the *IEEE TRANSACTIONS ON FUZZY SYSTEMS*, *Information Sciences*, *Swarm and Evolutionary Computation*, *Engineering Applications of Artificial Intelligence*, *IEEE/CAA JOURNAL OF AUTOMATICA SINICA*, *IEEE ACCESS* and *Journal of Intelligent and Fuzzy Systems*, and Co-Editor-in-Chief of *Journal of Artificial Intelligence and System*. He is the Leading Guest Editor of Special Issues in several prestigious journals, including *IEEE TRANSACTIONS ON EVOLUTIONARY COMPUTATION*, *IEEE TRANSACTIONS ON FUZZY SYSTEMS*, *IEEE TRANSACTIONS ON EMERGING TOPICS IN COMPUTATIONAL INTELLIGENCE*, *Information Fusion*, *Information Sciences*, *Applied Soft Computing*, etc. He has delivered more than 30 keynote speeches at international conferences and has served as the Program Chair, Workshop Chair, or Program Committee Member of several international conferences and symposiums in the area of data mining, fuzzy decision-making, and knowledge engineering, such as 2018 IEEE International Conference on Systems, Man, and Cybernetics, 2019 IEEE International Conference on Data Mining, 2019 IEEE Symposium Series on Computational Intelligence, 2019 IEEE Congress on Evolutionary Computation, 2019 International Joint Conference on Neural Networks, IEEE BigData 2020, 2020 IEEE International Conference on Fuzzy Systems, 2021 International Joint Conference on Neural Networks, 2021 IEEE Congress on Evolutionary Computation, 2021 International Joint Conference on Artificial Intelligence, etc.



Shouvik Chakraborty (Member, IEEE) received the B.Tech. degree in computer science and engineering from Hooghly Engineering and Technology College under the Maulana Abul Kalam Azad University of Technology (Formerly known as West Bengal University of Technology), Kolkata, India, and the M.Tech. degree in computer science and engineering in 2016 from the University of Kalyani, Kalyani, India, where he is currently working toward the Ph.D. (Former DST INSPIRE Fellow) degree in computer science and engineering.

He is currently a Lecturer with the Computer Science and Technology and In-charge, Robotics and Innovation Laboratory, M.B.C. Institute of Engineering and Technology (Government of West Bengal), Burdwan, India. His research interests include soft and evolutionary computing, digital image processing, biomedical image analysis, pattern recognition, machine learning, and optimization techniques.

Mr. Chakraborty was the recipient of the AICTE National Fellowship during the M.Tech. course and also class First position in M.Tech.



Kalyani Mali received the Bachelor's of Science (Hons.) degree in mathematics from the Lady Brabourne College, University of Calcutta, Kolkata, India, in 1983, the Bachelor of Technology (B. Tech.) and Master of Technology (M. Tech.) degrees in computer science from the University of Calcutta, Kolkata, India, in 1987 and 1989, respectively, and the Ph.D. degree in computer science from Jadavpur University, Kolkata, India, in 2005.

Her research interests include pattern recognition, digital image processing, data mining, soft computing

and multimedia. He is currently a Full Professor with the Department of Computer Science and Engineering, University of Kalyani, Kalyani, India.



Sankhadeep Chatterjee received the B. Tech degree in computer science and engineering from the Maulana Abul Kalam Azad University of Technology, Kolkata, India, in 2015, the M. Tech degree in computer science and engineering from the University of Calcutta, Kolkata, India, in 2017. He is currently working toward the Doctoral Research at the Indian Institute of Engineering Science and Technology, Shibpur, India.

He is currently an Assistant Professor with the University of Engineering and Management, Kolkata,

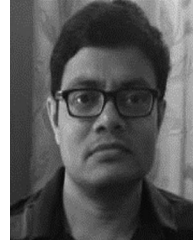
India. He obtained the prestigious Council of Scientific and Industrial Research Senior Research Fellowship from Government of India in 2019. He has authored or coauthored and presented more than 60 research papers in reputed International journals/conferences. His current research interests include machine learning, deep learning, metaheuristics, text data analysis, etc.



Janmenjoy Nayak received the Ph.D. degree in computer science and engineering from the Veer Surendra Sai University of Technology, Burla, Odisha, India, in 2017. He is currently an Associate Professor with the Department of Computer Science and Engineering, Aditya Institute of Technology and Management, Srikakulam, India. He has authored or coauthored more than 90 research papers in various reputed peer reviewed Referred Journals, International Conferences and Book Chapters. He was the Volume Editor of Series International Conference on Computational

Intelligence in Data Mining, Computational Intelligence in Pattern Recognition, etc. He has been a Guest Editor of various journal special issue from Elsevier, Springer and Inderscience. He has edited 9 books from various publishers, such as Elsevier and Springer. His research interest includes data mining, nature inspired algorithms and soft computing.

Mr. Nayak is the recipient of Best Researcher Award from the Jawaharlal Nehru University of Technology, Kakinada, Andhra Pradesh for the AY: 2018–2019, Young Faculty in Engineering-2017 Award by Venus International Foundation, Chennai. He is a Member of IEEE and a Life Member of some of the reputed societies, such as CSI India, etc.



Asit Kumar Das received the B.Tech. and M.Tech. degrees in computer science and engineering from the University of Calcutta, Kolkata, India, in 1996 and 2002, respectively, and the Ph.D. degree in engineering from Bengal Engineering and Science University Shibpur, Howrah, India, in 2011.

He is currently a Professor with the Department of Computer Science and Technology, Indian Institute of Engineering Science and Technology, Howrah, India. His subjects of interest include discrete structures, data structures and algorithms, database management systems, theory of computations, design and analysis of algorithms, data mining, and machine learning. He has authored or coauthored more than 100 research articles in peer-reviewed journals and international conferences. His current research interests include data mining and pattern recognition, social network analysis, evolutionary computing, and text, audio and video processing.

Dr. Das is the reviewer of several International Journals and has chaired many technical sessions in IEEE/Springer International conferences.



Soumen Banerjee (Senior Member, IEEE) received the B.Sc. (Hons.) degree in physics in 1998 from the University of Calcutta, Kolkata, India, where he received the B.Tech and M.Tech degrees in radio physics and electronics from the Institute of Radio Physics and Electronics, in 2001 and 2003 respectively, and the Ph.D. degree in engineering from the Indian Institute of Engineering Science and Technology, Howrah, India.

He is the Head-of-the-Department of Electronics of Communication Engineering, University of Engineering and Management, Kolkata, India. He was the Visiting Faculty with the Department of Applied Physics, University of Calcutta. He has a teaching/research experience of more than 20 years. His current research interests include design, fabrication and characterization of wide band gap semiconductor based Impatt diodes at D-band, W-band and THz frequencies, SIW technology based antennas, printed antennas and arrays, FSS, dielectric resonator antennas, body wearable antennas, machine learning, fuzzy systems and evolutionary computation. He has authored or coauthored more than 100 contributory papers in Journals and International Conferences. He has authored ten books and five book chapters in the fields of communication engineering, electromagnetic field theory, microwave and antenna. He has edited 3 books published by Springer. His profile is included in IBC, Cambridge, England and Marquis Who's Who in the World, USA.

Dr. Banerjee is a Senior Member of IEEE AP Society. He is also Fellow of IETE (New Delhi, India). He is the Reviewer of several International Journals like IEEE TRANSACTION ON EMERGING TOPICS IN COMPUTATIONAL INTELLIGENCE, IEEE TRANSACTION ON ELECTRON DEVICES, IEEE ACCESS, IEEE SENSORS LETTERS, MICROWAVE AND OPTICAL TECHNOLOGY LETTERS (MOTL-Wiley), *Journal of Electromagnetic Waves and Applications* (Taylor & Francis), *Radioengineering Journal* (Czech and Slovak Technical University), *Journal of Computational Electronics* (Springer-Nature), *Journal of Renewable and Sustainable Energy* (American Institute of Physics-AIP), *Cluster Computing* (Springer-Nature), *Journal of Infrared, Millimeter and Terahertz Waves* (Springer-Nature), etc. He was a Convener in International Conferences such as OPTRONIX-2019 (IEEE) and OPTRONIX-2020 (Springer); both held at Kolkata, India, and also chaired many technical sessions in several International Conferences.